Bulletin of Geophysics and Oceanography Vol. 65, n. 3, pp. 475-490; September 2024
DOI 10.4430/bgo00460

New additional boundary conditions for integrating a class of homogeneous models of wind-driven ocean circulation

F. Crisciani[1] and R. Mosetti[2]

[1] *Former Research Executive, ISMAR-CNR, Italy*
[2] *Former Research Executive, OGS-Trieste, Italy*

(Received: 23 January 2024; accepted: 4 April 2024; published online: 24 August 2024)

ABSTRACT A classical non-linear quasi-geostrophic model of wind-driven ocean circulation is integrated by using new additional boundary conditions conceived to: a) preserve, as far as possible, the typical structure of the Sverdrup flow in the southern and eastern regions of an idealised sub-tropical gyre and b) eliminate any additional boundary conditions in the northern and western regions of the fluid domain. Numerical simulations produce current and transport values close to those found in the literature whereas instability occurs at relatively low values of non-linearity, consistently with the well-known Sverdrup-like behaviour of large-scale transport in the world-wide ocean. A strict correlation emerges between the stability and the persistence of the Sverdrup-like behaviour of the so obtained solutions.

Key words: additional boundary conditions, wind-driven circulation, wind curl.

1. Introduction

Homogeneous models of wind-driven circulation have had a long history since the pioneering works of Stommel (1948) and Munk (1950) and they occupy a central role in the framework of geophysical fluid dynamics. In Pedlosky (1996), where a wide list of references is also found, the most relevant models are revisited and compared. More noticeably, in the same book, a still unresolved question is posed, that is on the lack of uniqueness of the additional boundary conditions demanded to carry out the integration of the quasi-geostrophic potential-vorticity equation governing most of these models. The problem arises whenever the dissipation of relative vorticity is parameterised in terms of its lateral diffusion (this characterises the class of models under investigation), thus raising the order of the quasi-geostrophic potential-vorticity equation to four, with the consequent need of further boundary conditions, besides those of no mass-flux, to single out a unique model solution. In Pedlosky (1996), different options are expounded and their influence on the resulting current field, in particular in the north-western region of the fluid domain, is illustrated. Already Blandford (1971) had highlighted the phenomenon in a set of numerical experiments.

This investigation addresses the problem concerning the choice of additional boundary conditions on the basis of the following criteria. The starting point is twofold: first, observational data [see, for instance, Welander (1959) and Wunsh (2011)] confirm the validity of the Sverdrup (1947) regime in the southern and eastern areas of real oceanic basins. Second, four 'identities' are inferred from the Sverdrup stream function evaluated from the wind-stress. Two of the

© 2024 - The Author(s)

'identities' concern linear and homogeneous relationships involving the derivatives of the stream function at the southern edge of the fluid domain (usually square), while the other two refer to the eastern edge. Then, four relationships having the same form as these 'identities', but written in terms of full model solution, are taken as additional boundary conditions at the same edges. Consistently, no additional condition for the remaining boundary part is introduced. At each edge, the two boundary conditions introduced are linearly independent and are determined implicitly by the wind-stress field. The aim is to obtain a model solution as close as possible to that of the Sverdrup flow in the region where observational data confirm its validity and not to impose additional conditions in the north-western part of the domain where the dynamics are 'poorly understood' (Pedlosky, 1991).

Numerical simulations are carried out with increasing non-linearity values with respect to a constant lateral dissipation, as far as the pattern of the Sverdrup flow emerges in the southern and eastern zones of the basin. Stable solutions yield velocity and transport values close to those found in the literature; in the case of non-linearity, sufficiently high unstable pseudo-solutions, which destroy the typical shape of the Sverdrup flow in the southern and eastern zones of the basin, appear. Section 2 reports the quasi-geostrophic potential-vorticity equation in the form used in what follows together with the new additional boundary conditions; Section 3 expounds the numerical experiments and results. In Section 4, the method is extended to a class of models with a wind-stress more general than the canonical.

2. The quasi-geostrophic potential-vorticity equation and boundary conditions

The wind-driven ocean circulation is, ultimately, the consequence of the alternation in latitude of the sign of the wind-stress, $\boldsymbol{\tau}$, over the ocean. In latitudinal intervals, where a single alternation takes place, the convergence/divergence of transport in the Ekman layer is compensated by a downward/upward vertical flow velocity that is proportional to the vertical component of the wind-stress curl. Thus, according to the Sverdrup balance, $curl_z \boldsymbol{\tau}$ is the forcing of the fluid columns in motion beneath the Ekman layer and down to the sea floor. This mechanism gives origin to the gyre-like structure of the oceanic current field. In the framework of the β- plane approximation, the evolution of the steady barotropic wind-driven current, **u**, can be expressed, in dimensionless form, by means of the quasi-geostrophic potential vorticity equation [standard notation as in Pedlosky (1987)]:

$$\left(\delta_I / L\right)^2 J\left(\psi,\ \nabla^2\psi\right) + \frac{\partial \psi}{\partial x} = curl_z \boldsymbol{\tau} + \left(\delta_M / L\right)^3 \nabla^4 \psi \tag{1}$$

where $\mathbf{u} = \hat{\mathbf{k}} \times \nabla\psi$. In the numerical simulations that follow, the inertial boundary layer width, d_I/L, is a variable parameter, while the frictional boundary layer width, δ_M/L, is maintained constant. Eq. (1) could be supplemented with the bottom friction term $-(\delta_S/L)\nabla^2\psi$ but in this context it is neglected as it is not strictly involved in the problem under investigation. Canonical wind-stress

$$\boldsymbol{\tau} = -\cos\left(\pi y\right)/\pi\ \hat{\mathbf{i}} \tag{2}$$

is used almost universally in wind-driven models and exhibits the desired alternation of its sign in interval $0 \le y \le 1$. Owing to Eq. (2), Eq. (1) becomes

$$\left(\delta_I / L\right)^2 J\left(\psi,\ \nabla^2\psi\right)+\frac{\partial\psi}{\partial x}=-\sin\left(\pi y\right)+\left(\delta_M / L\right)^3 \nabla^4\psi. \tag{3}$$

The isotropy of the horizontal length scales far from the boundaries suggests considering a fluid domain of the type

$$D=\left(0\le x\le 1\right)\times\left(0\le y\le 1\right). \tag{4}$$

The assumed impermeability of the domain boundary (4) implies the no mass-flux condition

$$\psi\left(x,y\right)=0\ \ \forall x,y\in\partial D. \tag{5}$$

The bi-harmonic term, $\nabla^4\psi$, of Eq. (3) demands the specification of a set of four other boundary conditions, named 'additional'. Additional boundary conditions (for instance, no-slip, free-slip, and super-slip) are expressed in terms of a linear and homogeneous differential operator, acting on the stream function, whose order is lower or equal to three, consistently with the fourth order of Eq. (3). Additional conditions have the linear and homogeneous form

$$\sum_{k=1}^{3} a_k \frac{\partial^k\psi}{\partial x^k}=0 \text{ in } x=0 \text{ and/or in } x=1 \tag{6}$$

and

$$\sum_{k=1}^{3} b_k \frac{\partial^k\psi}{\partial y^k}=0 \text{ in } y=0 \text{ and/or in } y=1. \tag{7}$$

Eqs. (6) and (7) are constraints on the meridional velocity (and its cross-stream derivatives) at the meridional edges and on the zonal velocity (and its cross-stream derivatives) at the zonal edges of the fluid domain (4). Reconsidering the dynamics, the Sverdrup stream function, associated to the wind-stress of Eq. (2) and in the fluid domain (4), is the solution to problem

$$\begin{cases} \dfrac{\partial\psi_{Sv}}{\partial x}=-\sin\left(\pi y\right) \\ \psi_{Sv}\left(1,y\right)=0 \end{cases} \tag{8}$$

that is

$$\psi_{Sv}=\left(1-x\right)\sin\left(\pi y\right). \tag{9}$$

Problem (8) is a limit version of Eq. (3) with Eq. (5) in which δ_I/L and δ_M/L are set to zero and the western side of the boundary is not considered. At this point, in the southern and eastern zones of the fluid domain, a Sverdrup balance is expected and this model aims to take into account this request as follows. Solution (9) satisfies two equations of the type (6) in $x = 1$ (i.e. in the eastern boundary) and two equations of the type (7) in $y = 0$ (i.e. in the south boundary), i.e.:

$$\left(\frac{\partial^2 \psi_{Sv}}{\partial x^2}\right)_{x=1} = 0 \tag{10}$$

$$\left(\frac{\partial^3 \psi_{Sv}}{\partial x^3}\right)_{x=1} = 0 \tag{11}$$

$$\left(\frac{\partial^2 \psi_{Sv}}{\partial y^2}\right)_{y=0} = 0 \tag{12}$$

$$\left(\frac{\partial^3 \psi_{Sv}}{\partial y^3} + \pi^2 \frac{\partial \psi_{Sv}}{\partial y}\right)_{y=0} = 0. \tag{13}$$

Indeed, Eqs. (10) and (11) are identities in x, but this fact is not important for the purposes of the foregoing developments. As anticipated in the introduction, the key point is that Eqs. (10) and (11), written in terms of full solution, are taken as additional boundary conditions to be applied to ψ (x, y) in the eastern boundary, that is to say:

$$\left(\frac{\partial^2 \psi}{\partial x^2}\right)_{x=1} = 0 \tag{14}$$

$$\left(\frac{\partial^3 \psi}{\partial x^3}\right)_{x=1} = 0. \tag{15}$$

In the same way, Eqs. (12) and (13) establish the additional boundary conditions of the full solution in the southern boundary, i.e.:

$$\left(\frac{\partial^2 \psi}{\partial y^2}\right)_{y=0} = 0 \tag{16}$$

$$\left(\frac{\partial^3 \psi}{\partial y^3} + \pi^2 \frac{\partial \psi}{\partial y}\right)_{y=0} = 0. \tag{17}$$

To summarise, the model to be integrated is given by Eq. (3), no mass-flux condition (5), and additional conditions (14) to (17).

Remark: keeping in mind Eqs. (5), (14), and (15), in the proximity of the eastern edge (x = 1) of the domain, the Taylor expansion of the model solution in powers of x = 1 provides:

$$\psi(x,y) = v(1,y) + \sum_{k\geq 4} \frac{1}{k!}\left(\frac{\partial^k \psi}{\partial x^k}\right)_{x=1} (x-1)^k \tag{18}$$

where v(1, y) is the meridional current at the eastern boundary. Conversely, the Sverdrup stream function can be written as:

$$\psi_{Sv}\left(x,y\right)=v_{Sv}\left(1,y\right)\left(x-1\right). \tag{19}$$

In the easternmost part of the fluid domain neither non-linearity nor dissipation yield a perceivable difference between the full solution and that of Sverdrup; thus, *a fortiori*, $v(1, y) = v_{Sv}(1, y)$. Hence, Eqs. (18) and (19) imply:

$$\psi(x,y)-\psi_{Sv}(x,y)=\sum_{k\geq 4}\frac{1}{k!}\left(\frac{\partial^k\psi}{\partial x^k}\right)_{x=1}(x-1)^k$$

and, therefore,

$$\lim_{x\to 1}\frac{\psi\left(x,y\right)-\psi_{Sv}\left(x,y\right)}{\left(x-1\right)^4}<\infty. \tag{20}$$

Limit (20) expresses the 'closeness' of the full solution to that of Sverdrup that, owing to Eqs. (10) and (11), extends from the eastern boundary westwards at every latitude. A similar analysis can be carried out in the proximity of the southern edge but limited to those longitudes where the phenomenological approximation

$$u\left(x,0\right)\approx u_{Sv}\left(x,0\right) \tag{21}$$

holds true. This due to the discrepancy between the zonal current, $u(x, 0)$, of the full solution and that of Sverdrup, $u_{Sv}(x, 0) = -\pi(1-x)$, which is unable to satisfy the no mass-flux at the western boundary. From Eqs. (5), (6), and (7), Taylor expansion

$$\psi\left(x,y\right)=-u\left(x,0\right)\left(y-\pi^2y^3/6\right)+R_4\left(y\right) \tag{22}$$

follows. In Eq. (22), $R_4(y)$ is the part of expansion (22) starting from y^4. Quite analogously, the Sverdrup stream function can be expanded, with the aid of Eqs. (12) and (13), to give

$$\psi\left(x,y\right)=-u\left(x,0\right)\left(y-\pi^2y^3/6\right)+Q_4\left(y\right) \tag{23}$$

where $Q_4(y)$ is the part of expansion (23) starting from y^4. Thus, limited to the longitudes where approximation (21) is acceptable, Eqs. (22) and (23) yield, in analogy with Eq. (20),

$$\lim_{y\to 0}\frac{\psi\left(x,y\right)-\psi_{Sv}\left(x,y\right)}{y^4}<\infty. \tag{24}$$

Relationships (20) and (24) mathematically express the idea of preserving, as far as possible, the Sverdrup flow in the south-eastern region of an idealised sub-tropical gyre, as anticipated.

3. Numerical experiments and results

3.1. Numerical scheme

Numerical models of wind-driven circulation based on centred-finite-difference methods date back to the pioneering work of Bryan (1963) up to the highest number of contributions listed, for instance, in Pedlosky (1996). By following this line, a numerical code is implemented to solve the full-time dependent version of the vorticity equation. The Jacobian term is evaluated using the Arakawa (1966) scheme, which conserves kinetic energy and enstrophy, while the relative vorticity is inverted using the method of successive over-relaxation. Integrations are performed on a specified domain with the proper boundary conditions. Particular attention is paid to the conversion of the new, and not standard, additional conditions (14) to (17) into the numerical scheme. The conversion is carried out by means of the ghost point method for the boundary region (Causon and Mingham, 2010). All the simulations are carried out on a spatial grid of 128×128 points and considering the dimensionless time step, that guarantees numerical stability.

3.2. Numerical simulations

As the main aim of any numerical approach in the quasi-geostrophic framework is to deal with non-linearity, whose degree is quantified in Eq. (2) by $(\delta_I/L)^2$, different values of $(\delta_I/L)^2$ are taken into account according to the following list:

	A	B	C	D
$10^4\left(\delta_I/L\right)^2$	1.6	3.0	3.5	4.0

(25)

while vorticity diffusion is maintained fixed, with $(\delta_M/L)^3 = 1.25\times10^{-4}$ by assuming $\delta_M = 5\times10^4$ m and $L = 10^6$ m. The isolines of the stream function and total vorticity $[q = (\delta_I/L)^2\nabla^2\psi + y]$ are depicted in each case, together with the time evolution of related energy $E = \int_D |\nabla\psi|^2 dxdy$.

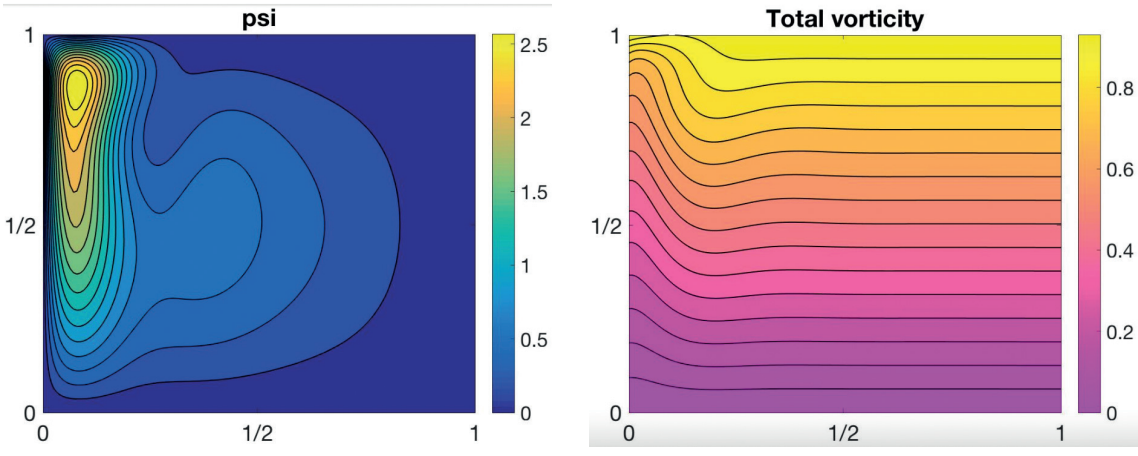

a b

Fig. 1 - Streamlines of case A (a); and isolines of the total vorticity of case A (b).

Case A is described in Fig. 1. Fig. 1a (contour of ψ) shows the typical northward shift of the gyre centre with respect to the linear case [already investigated by Badin *et al*. (2012)] and the formation of a return flow in proximity of the western boundary. The stream function maximum is ψ_{max} = 1.97. The contour lines reported in Fig. 1b (contour of q) stress the formation of a Sverdrup balance in a large part of the basin, with the obvious exception of its NW corner. In this case, current ($U = \beta \delta_I^2$) and transport ($M = ULH\psi_{max}$) are evaluated setting, as in Pedlosky (1987), $\beta = 10^{-11}$ m^{-1}s^{-1}, $H = 5\times10^3$ m whence

$$U = 1.6\times10^{-3} \text{ ms}^{-1}, \qquad M = 1.57\times10^{7} \text{ m}^3\text{s}^{-1}. \tag{26}$$

Case B is described in Fig. 2. Fig.2a shows the tendency of the gyre centre to move eastwards with respect to case A, with a weakening of the return flow. The stream function maximum is ψ_{max} = 2.44. The contour lines reported in Fig. 2b maintain marked evidence of the formation of a Sverdrup balance in a large part of the basin, but with wider undulations, as discussed by Cessi *et al*. (1990), and the consequent flux of total vorticity across the northern boundary not constrained by any additional boundary condition. In this case:

$$U = 3.0\times10^{-3} \text{ ms}^{-1}, \qquad M = 3.66\times10^{7} \text{ m}^3\text{s}^{-1}. \tag{27}$$

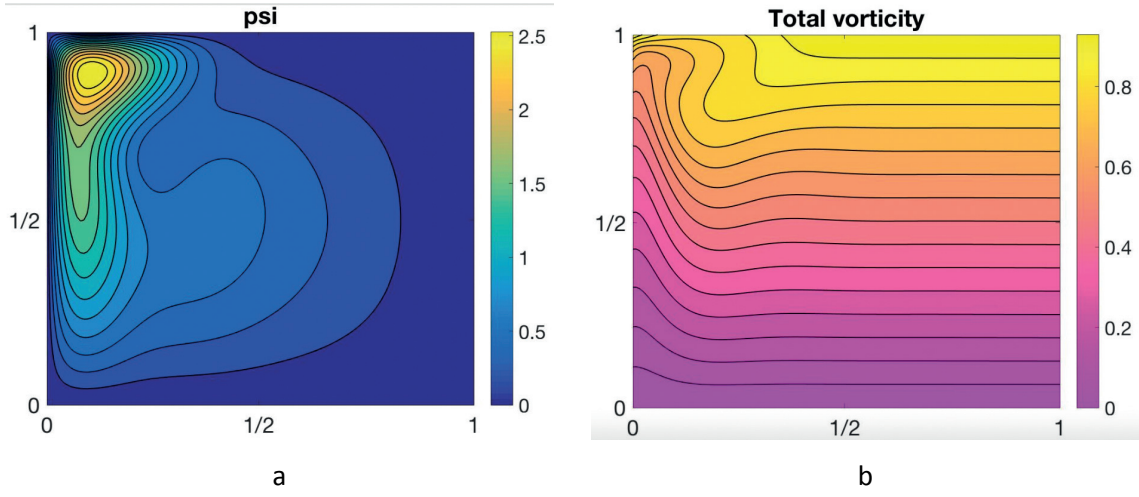

Fig. 2 - Streamlines of case B (a); and isolines of the total vorticity of case B (b).

Case C is described in Fig. 3. In Fig. 3a, the gyre centre moves further eastwards with respect to case B, without any remarkable difference. The stream function maximum is ψ_{max} = 2.66. The contour lines of Fig. 3b show even wider undulations with respect to case B and a larger eastward shift. However, the tendency of the formation of a Sverdrup balance is still evident in the eastern part of the basin. In this case

$$U = 3.5\times10^{-3} \text{ ms}^{-1}, \qquad M = 4.65\times10^{7} \text{ m}^3\text{s}^{-1}. \tag{28}$$

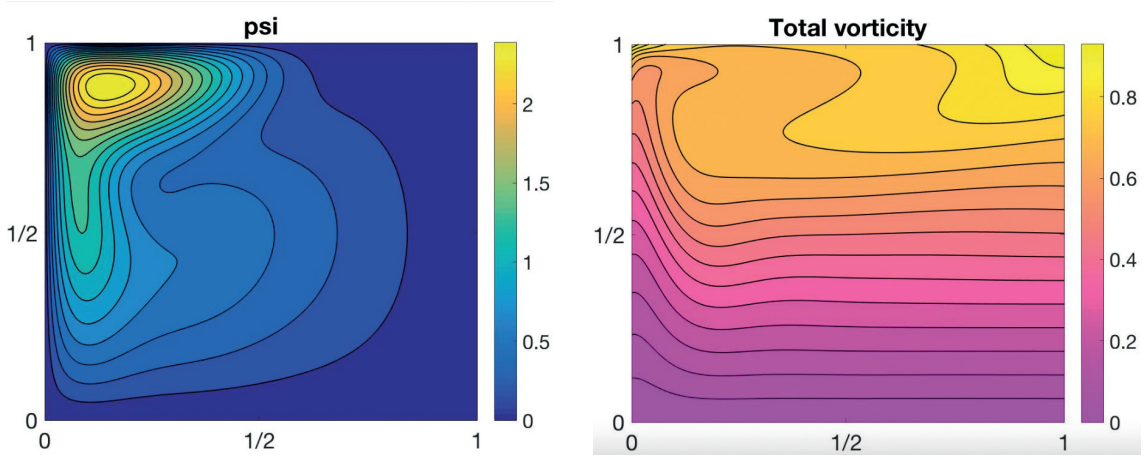

Fig. 3 - Streamlines of case C (a); and isolines of the total vorticity of case C (b).

This model, where $(\delta_i/L)^2 = 3.5\times10^{-4}$, seems to be very close to the threshold of instability, which is overcome in the following case D.

In all the above cases, a steady state is reached after a suitable final time of integration. This is confirmed by the behaviour of $E(t)$, computed for each case A, B, and C (Fig. 4).

In cases A, B, and C, the integrated enstrophy also converges to a constant value in time, proving the consistency of the numerical scheme even in the presence of the additional boundary conditions adopted here. Fig. 5 shows the plot of the integrated enstrophy versus time.

Outputs (26), (27), and (28) do not differ significantly from estimates

$U = 2\times10^{-3}$ ms^{-1}, $M = 3\times10^{7}$ m^{3}s^{-1}

cited in the literature (see Pedlosky, 1987, 1996).

Indeed, the circulation pattern of cases A, B, and C are not surprisingly different, for instance, from those reported in Boening (1986), Ierley (1987), and Carnevale *et al*. (2001).

In case D, convergence does not hold. The predominance of inertia, with respect to dissipation, brings the gyre centre towards the central longitude of the basin (Fig. 6a). At the same time, in the north-eastern corner of the domain, the total vorticity contours (Fig. 6b) are no longer consistent with the shape of the Sverdrup flow. Thus, the high instability, expressed by the divergence in time of $E(t)$, is in conflict with the additional conditions adopted to build up stable model solutions. This fact looks quite singular with respect to the customary framework in which additional conditions are left unaffected by the possible instability of the pseudo-solutions of the model [see, for instance, Cessi *et al*. (1990)]. A visual inspection of the streamlines of q for the stable solutions shows that the total vorticity gradient has a net northward component also in the area where non-linearity dominates (Figs. 1b, 2b, 3b). On the contrary, the snapshot obtained from an unstable pseudo-solution (Fig. 5b) points out a total vorticity gradient with a marked eastward component also in the area where $\nabla q \approx \hat{\mathbf{j}}$ is expected, in accordance with the Sverdrup solution. This qualitative aspect is supported by inequality (see the Appendix for its derivation):

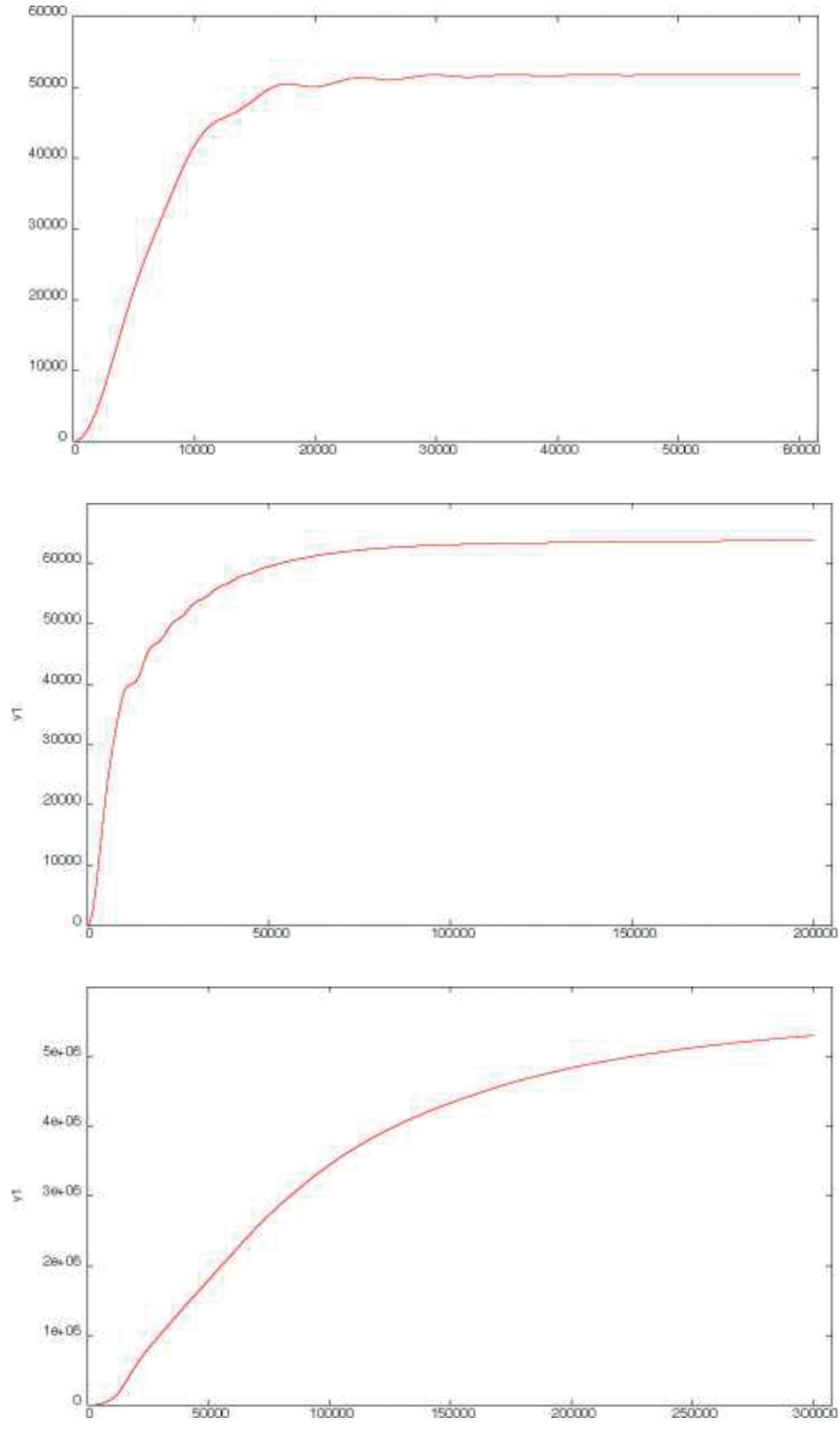

Fig. 4 - Plot of the integrated energy versus time for case A (upper panel), case B (central panel), and case C (lower panel). Worthy of notice is the fact that, in case C, the steady regime is reached on a much longer integration time with respect to cases A and B.

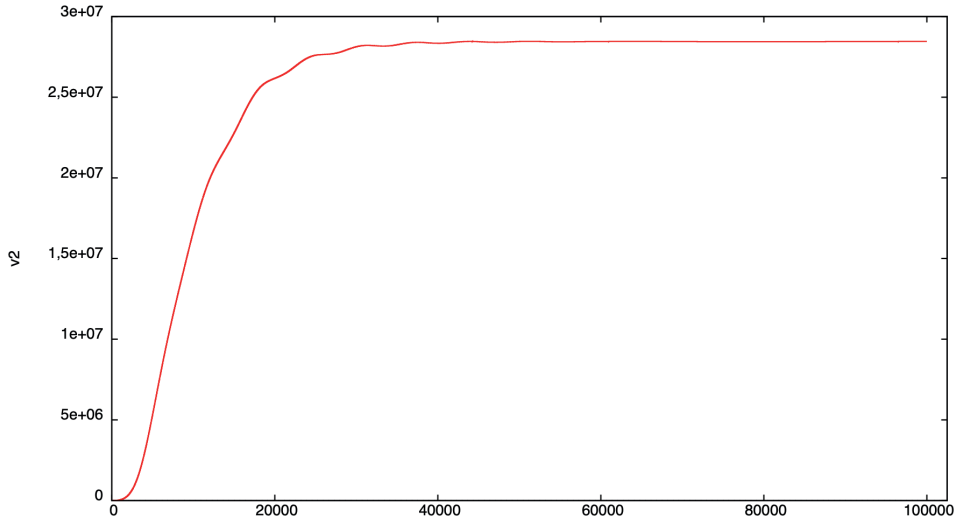

Fig. 5 - Integrated enstrophy versus time in case A.

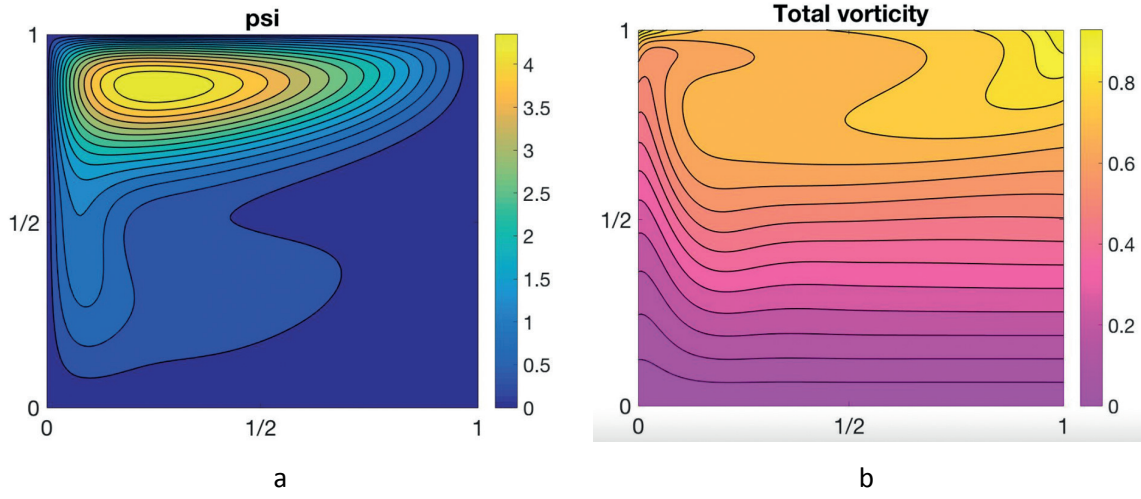

Fig. 6 - Snapshot of the streamlines of case D evaluated after time steps (a); and isolines of the total vorticity of case D under the same conditions (b).

$$\int_D \left|\nabla\psi\right|^2 dx\,dy \le \left(\frac{L}{\pi^2\delta_l}\right)^2 \int_D \left|\nabla q - \hat{\mathbf{j}}\right|^2 dx dy. \tag{29}$$

In fact, unstable pseudo-solutions imply the divergence in time of the energy on the left side of inequality (29) and, hence, the divergence of the 'distance', in the L_D^2-norm, of ∇q with respect to $\hat{\mathbf{j}}$ on the right side of the same inequality. In other words, instability implies an unlimited departure of ∇q from the northward direction.

4. A criterion to select the additional conditions for a wind-stress class

The stream function (9) is a special case of the Sverdrup stream function of the type

$$\psi_{Sv}\left(x,y\right)=\left(1-x\right)\frac{d\boldsymbol{\tau}}{dy} \tag{30}$$

where $\boldsymbol{\tau} = \tau(y)\,\hat{\mathbf{i}}$ takes the place of canonical wind-stress. The consideration of a more general wind-stress arises, for instance, due to the lack of symmetry north↔south in the shape of $\delta\tau/dy$ exhibited by zonal wind in most ocean basins. The presence of a single alternation of the sign of $\tau(y)$ in $0 \le y \le 1$ implies that $\tau(y)$ has an extreme in $y = 0$ (besides another in $y = 1$), so

$$\left(\frac{d^2\boldsymbol{\tau}}{dy^2}\right)_{y=0} \neq 0\,. \tag{31}$$

Inequality (31) will be useful in the cases that follow. Eq. (30) yields the below listed identities:

$$\begin{aligned}
&\frac{d^3\boldsymbol{\tau}}{dy^3}\frac{\partial\psi_{Sv}}{\partial y}-\frac{d^2\boldsymbol{\tau}}{dy^2}\frac{\partial^2\psi_{Sv}}{\partial y^2}=0\\
&\frac{d^4\boldsymbol{\tau}}{dy^4}\frac{\partial\psi_{Sv}}{\partial y}-\frac{d^2\boldsymbol{\tau}}{dy^2}\frac{\partial^3\psi_{Sv}}{\partial y^3}=0\\
&\frac{d^4\boldsymbol{\tau}}{dy^4}\frac{\partial^2\psi_{Sv}}{\partial y^2}-\frac{d^3\boldsymbol{\tau}}{dy^3}\frac{\partial^3\psi_{Sv}}{\partial y^3}=0
\end{aligned} \tag{32}$$

As in Section 2, Eq. (32) is written in terms of full solution ψ in place of ψ_{Sv} with reference only to the boundary in $y = 0$, that is to say

$$\left(\frac{d^3\boldsymbol{\tau}}{dy^3}\right)_{y=0}\left(\frac{\partial\psi}{\partial y}\right)_{y=0}-\left(\frac{d^2\boldsymbol{\tau}}{dy^2}\right)_{y=0}\left(\frac{\partial^2\psi}{\partial y^2}\right)_{y=0}=0 \tag{33a}$$

$$\left(\frac{d^4\boldsymbol{\tau}}{dy^4}\right)_{y=0}\left(\frac{\partial\psi}{\partial y}\right)_{y=0}-\left(\frac{d^2\boldsymbol{\tau}}{dy^2}\right)_{y=0}\left(\frac{\partial^3\psi}{\partial y^3}\right)_{y=0}=0 \tag{33b}$$

$$\left(\frac{d^4\boldsymbol{\tau}}{dy^4}\right)_{y=0}\left(\frac{\partial^2\psi}{\partial y^2}\right)_{y=0}-\left(\frac{d^3\boldsymbol{\tau}}{dy^3}\right)_{y=0}\left(\frac{\partial^3\psi}{\partial y^3}\right)_{y=0}=0 \tag{33c}$$

are taken as additional boundary conditions in $y = 0$. Indeed, only two equations of the set (33) are linearly independent, in fact (evaluation in $y = 0$ is understood).

$$\det\begin{pmatrix} d^3\tau/dy^3 & -d^2\tau/dy^2 & 0 \\ d^4\tau/dy^4 & 0 & -d^2\tau/dy^2 \\ 0 & d^4\tau/dy^4 & -d^3\tau/dy^3 \end{pmatrix} = 0.$$

Hence, the determination of the actual conditions to be applied in $y = 0$ is given by the following scheme:

	$\left(d^2\tau/dy^2\right)_{y=0}$	$\left(d^3\tau/dy^3\right)_{y=0}$	$\left(d^4\tau/dy^4\right)_{y=0}$
A	$\neq 0$	$\neq 0$	$\neq 0$
B	$\neq 0$	0	$\neq 0$
C	$\neq 0$	$\neq 0$	0
D	$\neq 0$	0	0

The first column is different to zero due to inequality (31). In row A, any couple of relationships among the set (33) gives appropriate additional boundary conditions. In row B, from Eqs. (33a) and (33c), the second term yields

$$\left(\frac{\partial^2\psi}{\partial y^2}\right)_{y=0} = 0 \tag{34}$$

while the first and third terms of the same row give the other condition, which is nothing but Eq. (33b). In row C, the third term implies from Eqs. (33b) and (33c):

$$\left(\frac{\partial^3\psi}{\partial y^3}\right)_{y=0} = 0 \tag{35}$$

while the first and second terms of the same row determine the condition expressed by Eq. (33a). Ultimately, case D selects conditions

$$\left(\frac{\partial^2\psi}{\partial y^2}\right)_{y=0} = 0 \tag{36}$$

$$\left(\frac{\partial^3\psi}{\partial y^3}\right)_{y=0} = 0. \tag{37}$$

In this way all the additional boundary conditions for a general stress of the type $\boldsymbol{\tau} = \tau(y)\,\hat{\mathbf{i}}$ are singled out. For instance, in interval $0 \le y \le 1$, stress $\boldsymbol{\tau} = -(1/\pi)(1-6y^2+4y^3)\,\hat{\mathbf{i}}$ is rather similar to that canonical in Eq. (2), however, here it is:

$$\left(d^2\tau/dy^2\right)_{y=0} = 12/\pi,\ \left(d^3\tau/dy^3\right)_{y=0} = -24/\pi,\ \left(d^4\tau/dy^4\right)_{y=0} = 0$$

and, therefore, case C applies, whence the additional boundary conditions on $y = 0$ result to be:

$$\left(\frac{\partial^3\psi}{\partial y^3}\right)_{y=0} = 0, \left(2\frac{\partial\psi}{\partial y} + \frac{\partial^2\psi}{\partial y^2}\right)_{y=0} = 0. \tag{38}$$

Boundary conditions (28) differ remarkably from boundary conditions (16) and (17) inferred for the canonical wind-stress in Eq. (2). Conversely, the validity of boundary conditions (14) and (15) is also retained for Eq. (30).

5. On longitude-dependent wind-stress

The criteria to select additional boundary conditions, expounded in Section 4, do not contemplate the case in which wind-stress also depends on longitude. This possibility was considered, for instance, by George Veronis (1966) who assumed[1]

$$curl_z \boldsymbol{\tau} = -\sin(\pi x)\sin(\pi y). \tag{39}$$

The point is that, in the current literature, there is no mention of canonical wind-stress, or one considered as such, that also depends on longitude. Consequently, this fact makes any attempt to deal with such wind-stress uncertain. Already in the original work of Sverdrup (1947) the author highlighted that, in the trade wind belt of the eastern Pacific, position $curl_z \boldsymbol{\tau} = -d\tau/dy$ was a good approximation of a total wind-stress *curl*. In any case, reconsidering Veronis (1966), additional boundary conditions can be actually inferred with the same method as that described in Section 2, noting that position (39) implies:

$$\psi_{Sv}(x,y) = [\cos(\pi x) + 1]\sin(\pi y)/\pi. \tag{40}$$

From solution (40), conditions (11), (12), and (13) again follow while the fourth boundary condition

$$\left(\frac{\partial\psi}{\partial x}\right)_{x=1} = 0 \tag{41}$$

is obtained in place of condition (10). This is due to the fact that factor $(1-x)$ of Eq. (9) is substituted by factor $[\cos(\pi x)+1]/\pi$ of solution (40).

6. Conclusions

This investigation aims to preserve, as far as possible, the Sverdrup flow in a class of non-linear quasi-geostrophic potential vorticity equations governing the wind-driven ocean circulation.

[1] Indeed, Veronis considered a bottom-dissipated model, thus, without introducing additional boundary conditions.

This is obtained by assuming the local Sverdrup solution in the southern and eastern zones of the subtropical gyre as a source of implicit conditions while leaving free from additional boundary conditions the western and northern edges.

A sketch of Pedlosky (1991), concerning the overall flow structure of an idealised subtropical gyre, has inspired the point of view expounded above. In the caption, this authoritative investigator claims: "In the southern and eastern zones, a Sverdrup balance is expected… In the north-western part of the gyre, a complex domain, poorly understood, is required to match to the interior". This explains the attempt to avoid the application of additional conditions in the north-western part of the gyre where the dynamics do not seem to be fully understood. Following this line, with a suitable numerical approach, a set of model solutions satisfying the so posed goal, has been obtained. A noticeable aspect lies in the fact that, by means of small variations of non-linearity, the model solutions look very similar to some classical ones reported in the literature and transport value *M* and current value *U* of the interior are very close to the estimates cited in the literature. Furthermore, instability arises for a relatively weak non-linearity with respect to lateral dissipation in accordance with the classical results inferred by observations in the world ocean.

REFERENCES

Arakawa A.; 1966: *Computational design for long-term numerical integration of the equations of fluid motion: two-dimensional incompressible flow, part I*. J. Comput. Phys., 1, 119-143, doi: 10.1016/0021-9991(66)90015-5.

Badin G., Barry A.M., Cavallini F. and Crisciani F.; 2012: *A new integration of Munk's linear model of wind-driven ocean circulation.* EPJ Plus, 127, 45-60.

Blandford R.R.; 1971: *Boundary conditions in homogeneous ocean models*. Deep Sea Res*.,* 18*,* 739-751.

Boening C.W.; 1986: *On the influence of frictional parameterization in wind- driven ocean circulation models*. Dyn. Atmos. Oceans, 10, 63-92.

Bryan K.; 1963: *A numerical investigation of a nonlinear model of a wind-driven ocean*. J. Atmos. Sci., 20, 594-606.

Carnevale G.F., Cavallini F. and Crisciani F.; 2001: *Dynamic boundary conditions revisited*. J. Phys. Oceanogr., 31, 2489-2497.

Causon D.M. and Mingham C.G.; 2010: *Introductory finite difference method for PDEs.* Bookboon, London, UK, 144 pp., <www.cs.man.ac.uk/~fumie/tmp/introductory-flnite-difference-methods-for-pdes.pdf>.

Cavallini F. and Crisciani F.; 2013: *Quasi-geostrophic theory of oceans and atmosphere*. Springer-Verlag, Berlin-Heidelberg, Germany, 385 pp.

Cessi P.R., Condie R.V. and Young W.R.; 1990: *Dissipative dynamics of western boundary currents.* J. Mar. Res., 48, 677-700.

Ierley G.R.; 1987: *On the onset of recirculation in barotropic general circulation models*. J. Phys. Oceanogr, 17, 2366-2374.

Munk W.H.; 1950: *On the wind-driven ocean circulation*. J. Meteor., 7, 79-93.

Pedlosky J.; 1987: *Geophysical fluid dynamics*. Springer-Verlag, Berlin-Heidelberg, Germany, 710 pp.

Pedlosky J.; 1991: *Theoretical developments in Ocean circulation theory*. Istituto Veneto di Scienze, Lettere ed Arti*,* Firenze Libri s.r.l., Reggello (FI), 124 pp.

Pedlosky J.; 1996: *Ocean circulation theory.* Springer-Verlag, Berlin-Heidelberg, Germany, 453 pp.

Stommel H.; 1948: *The westward intensification of wind-driven ocean currents*. Trans. Am. Geophys. Union, 29, 202-206.

Sverdrup H.U.; 1947: *Wind-driven currents in a baroclinic ocean; with applications to the equatorial current of the eastern Pacific.* Proc. Nat. Acad. Sci., 33, 318-326.

Veronis G.; 1966: *Wind-driven ocean circulation - Part 1. Linear theory and perturbation analysis*. Deep-Sea Res., 13, 17-29.

Welander P.; 1959: *On the vertically integrated mass transport in the oceans*. In: The atmosphere and the sea in motion. Ed. Bolin, B. Rockefeller Institute Press, New York, NY, USA, pp. 75-100.

Wunsch C.; 2011: *The decadal mean ocean circulation and Sverdrup balance*. J. Mar. Res., 69, 417-434.

Corresponding author: Renzo Mosetti
E-mail: rmosetti@gmail.com

Appendix: Proof of inequality (29)

The starting point is two versions of the Wirtinger inequality. The first one, based on boundary condition (5), is simply [see, for instance, Cavallini and Crisciani (2013)]:

$$\int_D \left|\nabla\psi\right|^2 dx\,dy \le \frac{1}{2\pi^2}\int_D \left(\nabla^2\psi\right)^2 dx\,dy. \tag{A1}$$

The second inequality presupposes boundary conditions

$$\left(\frac{\partial^2\psi}{\partial x^2}\right)_{x=1} = 0 \tag{A2}$$

and

$$\left(\frac{\partial^2\psi}{\partial y^2}\right)_{y=0} = 0 \tag{A3}$$

which are just ‘free-slip’ conditions (14) and (16), respectively. Due to Eq. (5), Eqs. (A2) and (A3) are, respectively, equivalent to:

$$\left(\nabla^2\psi\right)_{x=1} = 0 \tag{A4}$$

and

$$\left(\nabla^2\psi\right)_{y=0} = 0. \tag{A5}$$

Owing to Eq. (A4), the Wirtinger inequality yields

$$\int_0^1 \left(\nabla^2\psi\right)^2 dx \le \frac{4}{\pi^2}\int_0^1 \left(\frac{\partial}{\partial x}\nabla^2\psi\right)^2 dx$$

whence inequality

$$\int_D \left(\nabla^2\psi\right)^2 dx\,dy \le \frac{4}{\pi^2}\int_D \left(\frac{\partial}{\partial x}\nabla^2\psi\right)^2 dx\,dy \tag{A6}$$

immediately follows. Similarly, due to Eq. (A5), inequality

$$\int_D \left(\nabla^2\psi\right)^2 dx\,dy \le \frac{4}{\pi^2}\int_D \left(\frac{\partial}{\partial y}\nabla^2\psi\right)^2 dx\,dy \tag{A7}$$

can be inferred. Addition of inequality (A6) with inequality (A7) gives, after a trivial computation, inequality

$$\int_D \left(\nabla^2\psi\right)^2 dx\,dy \le \frac{2}{\pi^2}\int_D \left[\left(\frac{\partial}{\partial x}\nabla^2\psi\right)^2 + \left(\frac{\partial}{\partial y}\nabla^2\psi\right)^2\right] dx\,dy$$

that is to say

$$\int_D \left(\nabla^2\psi\right)^2 dx\,dy \le \frac{2}{\pi^2}\int_D \left|\nabla\left(\nabla^2\psi\right)^2\right| dx\,dy\,. \tag{A8}$$

Now, total vorticity implies

$$\nabla\left(\nabla^2\psi\right) = \left(L/\delta_I\right)^2 \nabla\left(q - y\right) = \left(L/\delta_I\right)^2 \left(\nabla q - \hat{\mathbf{j}}\right) \tag{A9}$$

so, substitution of Eq. (A9) into inequality (A8) results in inequality

$$\int_D \left(\nabla^2\psi\right)^2 dx\,dy \le 2\left(\frac{L}{\pi\delta_I}\right)^2 \int_D \left|\nabla q - \hat{\mathbf{j}}\right|^2 dx\,dy \tag{A10}$$

At this point, from inequalities (A1) and (A10), final inequality

$$\int_D \left|\nabla\psi\right|^2 dx\,dy \le 2\left(\frac{L}{\pi\delta_I}\right)^2 \int_D \left|\nabla q - \hat{\mathbf{j}}\right|^2 dx\,dy$$

is easily obtained.